https://doi.org/10.18321/ectj792

Control of Porphyrin Dye Aggregation Using Bis(4-pyridyl)Alkanes in Dye Sensitized Solar Cells

B. Baptayev[1,2], A. Rysbekova[2], D. Kalpakov[2], A. Aukenova[2], D. Mustazheb[2], Z. Salkenova[2], M. Kazaliyev[2], M. Balanay[2]*

[1]National Laboratory Astana, Kabanbay Batyr Ave. 53, Astana, Kazakhstan
[2]Nazarbayev University, Kabanbay Batyr Ave. 53, Astana, Kazakhstan

Article info

Received:
4 September 2018

Received in revised form:
13 October 2018

Accepted:
10 December 2018

Abstract

The aggregation of sensitizer molecules on the surface of photoanode is a serious issue that can affect the photovoltaic performance of dye-sensitized solar cells. Prevention of dye agglomeration, therefore, is critical. Traditional methods of aggregation control are either synthetically challenging or technologically difficult and expensive. In this article, the use of bis(4-pyridyl)alkanes to control porphyrin dye aggregation is presented. Three bis(4-pyridyl)alkanes – bis(4-pyridyl)butane L4, bis(4-pyridyl)octane L8 and bis(4-pyridyl)decane L10 were synthesized. These bis(4-pyridyl)alkane ligands are axially attached to the metallic center of synthesized porphyrin dye P. The complexes was obtained by mixing the solutions of dye P and each ligand (L) in 2:1 ratio 1 h before the soaking step. As a result three cells were prepared: P-L4, P-L8 and P-L10. The performance of these cells were compared with a reference cell which was prepared from porphyrin dye P only. IPCE analysis demonstrated the highest dye load in P-L4 cell which was ascribed to lowered dye aggregation. Photovoltaic analysis showed improved short circuit current density due to suppressed dye aggregation caused by the complexation of the porphyrin dye P with the linker L4. As a result the overall cell efficiency increased to 42% demonstrating the successful utilization of the (4-pyridyl)alkane linker complexes with porphyrin dye.

1. Introduction

Energy is a crucial element of human life. The increasing population and growing economy requires more energy. The use of fossil fuels as energy source has drawbacks due to environmental effects and supply limitations. Therefore, it is critical to search for sustainable sources of energy. Sunlight is one of green and renewable sources of energy which can fully satisfy the energy demand of whole planet [1]. Dye sensitized solar cells (DSSCs) represent third-generation solar cells and are regarded as low cost, high efficiency and easily prepared cells [2]. The current highest record efficiency of DSSCs is 13% which was obtained using porphyrin dye SM315 [3]. Porphyrins are unique dyes due to their strong absorption around 450 nm and 600–650 nm. They have great electron donating-accepting properties which is important for the sensitizers. Also, porphyrins have several positions that various substituents can be attached to. Unlike DSSCs made of Ru-dyes, the efficiency of porphyrin sensitized solar cells has been constantly increasing since 1990s [4]. One of the drawbacks of porphyrin dyes is their tendency to aggregate on semiconductor surface. Dye aggregation on semiconductor surface is a serious issue that needs to be prevented for the efficient performance of dye sensitized solar cells (DSSCs). The aggregation of sensitizers decreases the charge injection kinetics. Photoexcited aggregated molecules do not participate in electron injection due to charge annihilation. Moreover, dye aggregation may cause increased charge recombination with dye cation [5]. Porphyrins, a well-known class of DSSC sensitizers, also tend to aggregate on photoanode surface due to the planarity of its macrocycle [6]. Methods of aggregation control include

*Corresponding author. E-mail: mannix.balanay@nu.edu.kz

the incorporation of bulky groups on dye structure which can be synthetically challenging and/or the use of co-adsorbents that requires preparation of cocktail with optimal ratio. In this research, the authors present the use of bis(4-pyridyl)alkanes as effective spacers between porphyrin dyes that prevent dye aggregation by axially coordinating them with the dye metal atom. This allows the use of dyes with no bulky groups which simplifies the synthetic protocol and makes possible to control the distance between sensitizer molecules.

2. Experimental

Commercially available chemicals were obtained from Sigma Aldrich and Thermo Fisher Scientific. Some solvents, like pyrrole, were purified using rotary evaporator before use in synthesis. Most of the synthesis reactions are sensitive to moisture and oxygen, and, thus, reactions were performed in the inert atmosphere of nitrogen. Chemical structures of the synthesized products were confirmed via NMR spectroscopy method on JEOL JNM-ECA Series FT NMR spectrometer.

2.1. Synthesis of porphyrin dye

Porphyrin dye P was synthesized according to the scheme shown in Fig. 1.

2,2'–dipyrromethane (1). Formaldehyde (1.5 g, 50 mmol) was dissolved in purified pyrrole (347 ml, 5 mol) in round-bottom flask stirring for 10 min with purging nitrogen. Then, temperature of solution was increased to 55 °C and $InCl_3$ (1.1 g, 5 mmol) was added to stirring solution. After 2.5 h, NaOH (6 g, 0.15 mol) was added to the reaction mixture. Reaction was stopped after 1 h and cooled down to room temperature. Solution was filtrated, and solvent was evaporated using rotary evaporator. Thin-layer chromatography (TLC) showed presence of 3 products. Using column chromatography, three products of the reactions were separated and via NMR 2,2'-dippyromethane (white solid) was identified.

5,15–diphenylporphyrin (2). 2,2'-dippyromethane (1.48 g, 10 mmol) and benzaldehyde (1.03 ml, 10 mmol) were dissolved in anhydrous dichloromethane (DCM) and stirred at room temperature for 30 min. Trifluoroacetic acid (TFA) was added and stirring continued at inert atmosphere of nitrogen. After 3 h 2,3-dichloro-5,6-dicyano-1,4-benzoquinone (DDQ) was added, and after 15 min, 50 mmol of triethylamine (TEA) was added and stirring continued for 1 h. Reacting mixture was filtered and obtained products were separated by column chromatography. Solvent was evaporated and structure of product was confirmed.

10,20-dibromo-5,15–diphenylporphyrin (3). 5,15–diphenylporphyrin (750 mg, 1.6 mmol) was dissolved in anhydrous DCM and stirred at room temperature for 10 min. Then, temperature of the reaction was decreased to 0 °C in ice bath for

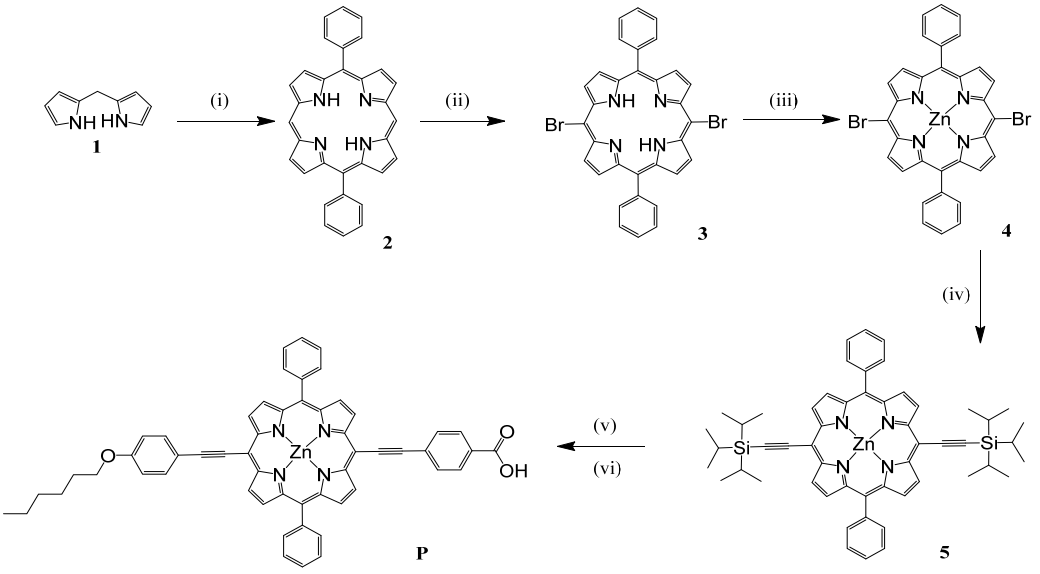

Fig. 1. Synthetic scheme of porphyrin dye (P). (i) C_6H_5CHO, CH_2Cl_2, TFA, DDQ, TEA, r.t.; (ii) CH_2Cl_2, r.t. → 0 °C, NBS; (iii) $CH_3COOZn{\cdot}2H_2O$, CH_2Cl_2, CH_3OH; (iv) TIPS, CuI, THF, TEA, $Pd(PPh_3)_2Cl_2$, r.t. → 85 °C; (v) TBAF, THF, p-IC_6H_4COOH, TEA, $Pd_2(dba)3$, $AsPh_3$, *p*-$C_6H_{13}OC_6H_4I$.

further addition of NBS (N-bromosuccinimide) (313 mg, 1.7 mmol). Reaction was quenched by adding acetone after 6 h. Solvent was evaporated and product was separated from by-products in column chromatography.

Zinc-10,20-dibromo-5,15–diphenylporphyrinate (4). 10,20-dibromo-5,15–diphenylporphyrin (270 mg, 3.7 mmol) and zinc acetate (1.3 g, 37 mmol) were dissolved in the mixture of DCM and methanol and stirred at room temperature for 3 h. Reaction was quenched by adding excess water. Aqueous and organic phases were separated in separatory funnel and organic phase were washed several times with DI water, dried over $MgSO_4$ and rotovapped to produce desired product.

Zinc-10,20-bis(triisopropylsilylethynyl)-5,15–diphenylporphyrinate (5). Metallated porhyrin (4) (500 mg, 0.731 mmol), (triisopropylsilyl)acetylene (870 mg, 3.87 mmol) and copper (I) iodide (14 mg, 0.0731 mmol) were dissolved in tetrahydrofuran (THF) in round-bottom flask with constant stirring in inert nitrogen atmosphere. TEA (5 ml) was added when solution became homogeneous. After purging nitrogen to reaction system for 20 min $Pd(PPh_3)_2Cl_2$ (51.7 mg, 0.0731 mmol) was added. Temperature of reacting mixture was increased to 85 °C and left overnight. Solvent was evaporated and product was separated using column chromatography.

5,15-diphenyl-10-(4-oxyhexylphenylethynyl)-20-(4-carboxyphenylethynyl)porphyrinatato zinc (P). Tetrabutylammonium fluoride (4.9 ml, 10.2 mmol) was added to compound 5 (0.9 g, 1.02 mmol) dissolved in THF and stirred for 2 h. Then, mixture of DCM and water was added to reacting mixture to produce aqueous and organic layers. Organic layer was separated and solvent was evaporated to produce intermediate product. 4-iodobenzoic acid (1.19 g, 4.8 mmol), TEA (5 ml), $Pd_2(dba)_3$ (0.19 g, 20 umol), triphenylarsine (2.5 g, 8 mmol) and 4-oxyhexyl iodobenzene (1.48 g, 4.8 mmol) were added to the intermediate compound (2.1 g) dissolved in THF. Reacting mixture stirred for 5 h in nitrogen atmosphere at 85 °C, and then cooled to room temperature and solvent was evaporated. Products of reaction were separated using column chromatography and structure of desired product was confirmed by NMR.

2.2. Synthesis of the linkers

The linkers were synthesized according to the scheme shown in Fig. 2.

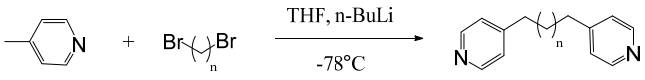

Fig. 2. Synthesis scheme of the linkers.

Bis(4-pyridyl) alkane. 4-methylpyridine (1.57 ml) was dissolved in THF and temperature of the solution was decreased to -83.6 °C in ethyl acetate – liquid nitrogen bath. n-butyllithium (13.1 g) was added to the solution dropwise and reaction stirred for 2 h. Then, 10 ml of THF was added and temperature of mixture was again decreased to -83.6 °C and dibromoalkane ligand (1.1 ml) was added dropwise (ligands: L4 – 1,4-dibromobutane, L8 – 1,8-dibromooctane and L10 – 1,10-dibomodecane). Reacting mixture was left stirring for 24 h. Reaction was quenched by adding 10 ml water. Organic layer was separated and solvent was evaporated. TLC shows three spots, indicating 3 products of the reaction, which are separated using column chromatography and NMR confirms the structure of desired product.

2.3. DSSC fabrication

Transparent TiO_2 paste (Dyenamo DN-EP03) was applied on the pre-treated with 40 mM $TiCl_4$ fluorine-doped tin oxide (FTO) glass by doctor blading and allowed to air dry for 2 h. Then the film was sintered stepwise in the oven (125 °C – 5 min, 325 °C – 10 min, 425 °C – 15 min, 500 °C – 30 min). After cooling it was again treated with 40 mM $TiCl_4$ and paste prepared from P25 (Aldrich 718467) was applied on top as scattering layer which was followed by stepwise sintering in the oven. The cooled films were post-treated with 40 mM $TiCl_4$ and finally sintered at 500 °C for 30 min. The cooled electrodes were soaked with 0.2 mM dye (P)/dye-linker (P:L (2:1) where dye concentration is 0.2 mM) solutions in dichloromethane-methanol (10:1) solutions for 4 h in refrigerator before assembling into DSSC using counter electrode and electrolyte. The counter electrode was made of platinum (Dyenamo DN-EP01) and the electrolyte was iodine/iodide based solution (Dyenamo DN-OD05).

2.4. Characterization

The photovoltaic performance was analyzed using Dyenamo Toolbox (DN-AE01). Incident-photon-to-current-conversion-efficiency graphs were obtained using Dyenamo IPCE Toolbox (DN-AE03). UV-Vis spectra were collected from

ThermoScientific Evolution 60S UV-Visible Spectrophotometer. The optimized structures were done in Gaussian 16 [7] using M06-2X hybrid functional [8] and Pople's split-valence double-zeta basis set with added d polarization function on non-hydrogen atoms.

3. Results and discussion

The obtained porphyrin dye P was analyzed by UV/Vis spectroscopy to observe its light absorption characteristics in dichloromethane-methanol (10:1) solution (Fig. 3). The dye P has two maximums: strong absorption at 451 nm and moderate light harvest at 660 nm.

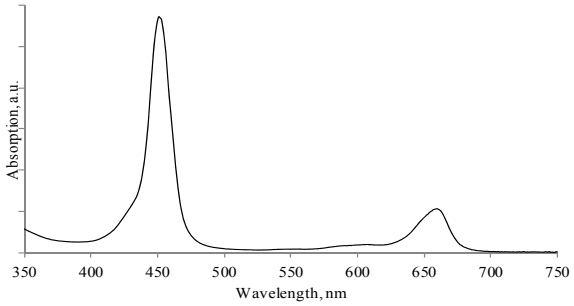

Fig. 3. UV/Vis absorption spectra of the porphyrin dye P.

The optimized structures were obtained from computational analysis performed using Gaussian 16 program as shown in Fig. 4. The analysis allowed to calculate the distance between two complexed porphyrin planes. Porphyrins are separated by 15.7 A° in P-L4 complex, the shortest distance due to the linker size. For P-L8 the distance is 20.4 A° and it further increases to 22.8 A° for P-L10 complex as the linker gets bigger.

Incident-photon-to-current-conversion-efficiency (IPCE) of the cells is shown in Fig. 5. This parameter shows how effective the dyes are in converting the absorbed photon into current. Two regions can be distinguished: around 450 nm and 680 nm which correspond to UV/Vis absorption data of the dye solutions (see Fig. 3.). It is clearly observable that cell P-L4 has the highest IPCE value indicating lowered aggregation and also higher dye load. This could be due to better complexation of the linker L4 with the porphyrin dye P compared to others. On the other hand the linker L4 is the shortest in length and therefore it occupies less space compared to other dye-linker complexes which gives higher chance for the P-L4 complex to attach to TiO_2 surface. This was confirmed by optimized structures of porphyrin-ligand complexes (Fig. 4.).

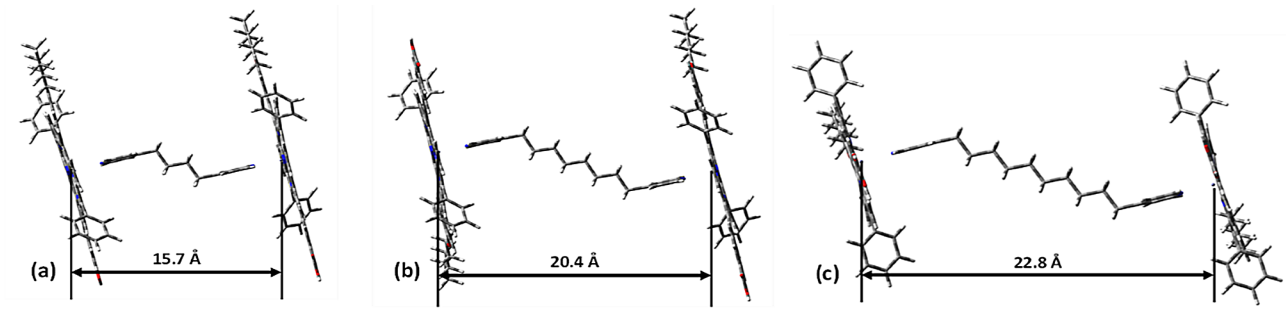

Fig. 4. Optimized structures of porphyrin-ligand calculated in M06-2X/6-31G(d) in vacuum: (a) – with (4-pyridyl) butane; (b) – (4-pyridyl)octane, and (c) – (4-pyridyl)decane. Also shown are the Zn-Zn distance between porphyrin analogues.

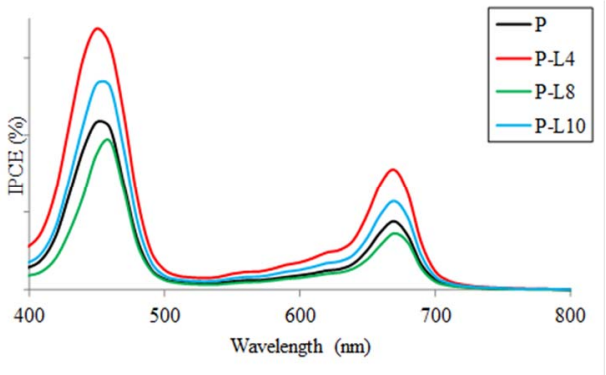

Fig. 5. IPCE spectra of the cells.

Photovoltaic performance of the dyes is presented in Fig. 6 and the corresponding data is shown in Table. I-V characteristics demonstrated the same trend similar to IPCE (see Fig. 5). Due to maximum IPCE value, the complex P-L4 produced the highest current, 3.23 mA/cm^2, among all samples. The improvement in Jsc value reached over 40% compared to the reference cell P with Jsc equal to 2.27 mA/cm^2, indicating suppressed dye aggregation in P-L4. P-L10 complex showed similar performance to reference cell P with small increase in Jsc following the trend in IPCE. The cell with dye

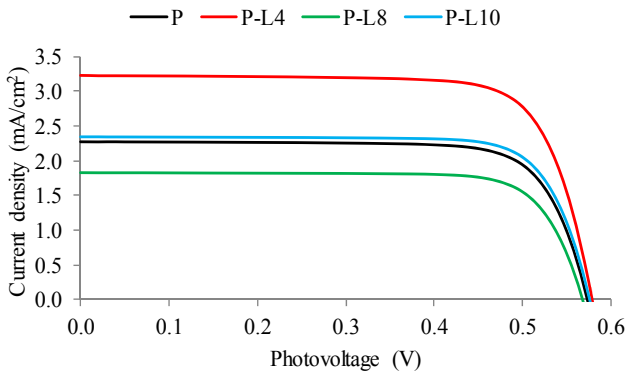

Fig. 6. I-V characterization of the cells.

complex P-L8 produced the lowest current of all. This was explained by the low IPCE value of the system among all samples. Unlike current density, the photovoltages and fill factors of the cells were found to be the same. The photovoltaic parameters are shown in Table. The highest current of P-L4 led to the highest efficiency among all samples – 1.42%, indicating 42% improvement and confirming the beneficial effect of the L4 linker in suppressing dye aggregation.

Table

Photovoltaic parameters of the cells

	Eff (%)	Voc (V)	Jsc (mA/cm^2)	FF
P	1.00	0.57	2.27	0.77
P – L4	1.42	0.58	3.23	0.76
P – L8	0.80	0.57	1.83	0.78
P – L10	1.05	0.58	2.34	0.77

4. Conclusions

Thus, this work demonstrated the use of bis(4-pyridyl)alkane linkers axially attached to porphyrin dye P in suppressing the dye aggregation. Three linkers were synthesized together with porphyrin dye. Porphyrin-linker complexes were prepared in 2:1 ratios with final dye concentration 0.2 mM. The photovoltaic measurements showed the improvement in current density in P-L4 complex leading to 42% improvement of cell efficiency. The increase in Jsc was ascribed to lowered dye aggregation which led to improved IPCE value of the cell compared to reference cell.

Acknowledgments

This research was funded under the program AP05134515 "Natural carbon dots as counter electrodes for photovoltaic applications" from the Ministry of Education and Science of the Republic of Kazakhstan.

References

[1]. E. Kabir, P. Kumar, S. Kumar, A.A. Adelodun, Ki-Hyun Kim, *Renew. Sust. Energ. Rev.* 82 (2018) 894–900. DOI: 10.1016/j.rser.2017.09.094

[2]. B. O'Regan, M. Grätzel, Nature 353 (1991) 737–740. DOI: 10.1038/353737a0

[3]. S. Mathew, A. Yella, P. Gao, R. Humphry-Baker, B.F.E. Curchod, N. Ashari-Astani, I. Tavernelli, U. Rothlisberger, Md. Khaja Nazeeruddin, M. Grätzel, *Nat. Chem.* 6 (2014) 242–247. DOI: 10.1038/nchem.1861

[4]. Lu-Lin Li and Eric Wei-Guang Diau, *Chem. Soc. Rev.* 42 (2013) 291–304. DOI: 10.1039/C2CS35257E

[5]. H. Matsuzaki, T.N. Murakami, N. Masaki, A. Furube, M. Kimura, S. Mori, *J. Phys. Chem. C* 118 (2014) 17205–17212. DOI: 10.1021/jp500798c

[6]. Hsueh-Pei Lu, Chen-Yuan Tsai, Wei-Nan Yen, Chou-Pou Hsieh, Cheng-Wei Lee, Chen-Yu Yeh, Eric Wei-Guang, *J. Phys. Chem. C* 113 (2009) 20990–20997. DOI: 10.1021/jp908100v

[7]. Gaussian 16, Revision A.03, M.J. Frisch, G.W. Trucks, H.B. Schlegel, G.E. Scuseria, M.A. Robb, J.R. Cheeseman, G. Scalmani, V. Barone, G.A. Petersson, H. Nakatsuji, X. Li, M. Caricato, A.V. Marenich, J. Bloino, B.G. Janesko, R. Gomperts, B. Mennucci, H. P. Hratchian, J.V. Ortiz, A.F. Izmaylov, J.L. Sonnenberg, D. Williams-Young, F. Ding, F. Lipparini, F. Egidi, J. Goings, B. Peng, A. Petrone, T. Henderson, D. Ranasinghe, V.G. Zakrzewski, J. Gao, N. Rega, G. Zheng, W. Liang, M. Hada, M. Ehara, K. Toyota, R. Fukuda, J. Hasegawa, M. Ishida, T. Nakajima, Y. Honda, O. Kitao, H. Nakai, T. Vreven, K. Throssell, J.A. Montgomery, Jr., J.E. Peralta, F. Ogliaro, M.J. Bearpark, J.J. Heyd, E.N. Brothers, K.N. Kudin, V.N. Staroverov, T.A. Keith, R. Kobayashi, J. Normand, K. Raghavachari, A.P. Rendell, J.C. Burant, S.S. Iyengar, J. Tomasi, M. Cossi, J.M. Millam, M. Klene, C. Adamo, R. Cammi, J.W. Ochterski, R.L. Martin, K. Morokuma, O. Farkas, J.B. Foresman, and D.J. Fox, Gaussian, Inc., Wallingford CT, 2016.

[8]. Y. Zhao, D.G. Truhlar. *Theor Chem Account*, 120 (2008) 215–241.DOI: 10.1007/s00214-007-0310-x